Applied Surface Science xxx (2014) xxx–xxx

Contents lists available at ScienceDirect

Applied Surface Science

journal homepage: www.elsevier.com/locate/apsusc

Orthogonal synthesis, structural characteristics, and enhanced visible-light photocatalysis of mesoporous Fe_2O_3/TiO_2 heterostructured microspheres

Ting Wang[a], Guidong Yang[a,*], Jia Liu[a], Bolun Yang[a,b], Shujiang Ding[c,**], Zifeng Yan[d], Tiancun Xiao[e]

[a] Department of Chemical Engineering, School of Chemical Engineering and Technology, Xi'an Jiaotong University, Xi'an, 710049, China
[b] State Key Laboratory of Multiphase Flow in Power Engineering, Xi'an Jiaotong University, Xi'an, 710049, China
[c] Department of Applied Chemistry, School of Science, Xi'an Jiaotong University, Xi'an, 710049, China
[d] State Key Laboratory for Heavy Oil Processing, China University of Petroleum, Qingdao, 266555, China
[e] Department of Chemistry, Inorganic Chemistry Laboratory, University of Oxford, Oxford, OX1 3QR, UK

ARTICLE INFO

Article history:
Received 18 March 2014
Received in revised form 10 May 2014
Accepted 11 May 2014
Available online xxx

Keywords:
Mesoporous
Fe_2O_3/TiO_2
Microsphere
Heterostructure
Photocatalysis
Visible-light

ABSTRACT

In this paper, a facile solvothermal method assisted orthogonal experimental was applied to synthesis mesoporous Fe_2O_3/TiO_2 heterostructured microsphere with the purpose of optimizing the preparation conditions. The as-prepared samples were characterized by TG, XRD, SEM, TEM, FT-IR, UV–vis DRS and N_2 adsorption/desorption. On the basis of the above analysis, it was found that the mesoporous Fe_2O_3/TiO_2 heterostructured microsphere has high crystallinity, ordered morphology, strong optical absorption, large surface area and enhanced catalytic activity. Furthermore, it also confirmed that orthogonal experimental design method was very efficient to optimize the preparation conditions for the synthesis of mesoporous Fe_2O_3/TiO_2 heterostructured microspheres. The experimental results show that the reaction temperature and molar ratio of Fe to Ti have the most influence on the photocatalytic performance. The optimized preparation conditions for the synthesis of Fe_2O_3/TiO_2 microspheres are reaction temperature at 140 °C, the amount of glucose of 3.4 g and the Fe:Ti molar ratio of 0.005:0.01. What's more, a tentative formation mechanism of mesoporous Fe_2O_3/TiO_2 microspheres and charge transfer mechanism are proposed.
© 2014 Elsevier B.V. All rights reserved.

1. Introduction

Since 1972, Fujishima and Honda reported that H_2O could be decomposed into hydrogen with titanium oxide (TiO_2) electrode under UV light irradiation, the utilization of semiconductor photocatalysts to address the environmental pollution problem and the global energy supply issue (e.g. the generation of hydrogen and solar cell) have been widely drawn much attentions [1–6]. It is known that photocatalysis is the use of UV or visible light to active photocatalysts, such as TiO_2 semiconductors, that can potentially oxidize various organic compounds in air or water [7], and this method is considered as a promising environmental remediation technology, especially for the removal of low levels of organic contaminants.

Titanium oxide (TiO_2), a well-known photocatalytic material, possesses unique physicochemical properties of low cost, non-toxicity, excellent stability and high photocorrosion resistance [7,8], and which has been extensively investigated in the field of environmental purification, solar energy conversion and hydrogen generation [9–11]. Additionally, the architectural structure of the photocatalyst was proved to be an important factor for the higher catalytic activity because most catalytic reactions occurred on the catalyst surface. Thus, a variety of controlled synthesis methods have been attempted to synthesize well-defined particles morphology, such as monodisperse nanoparticles, mesoporous microspheres, macro/mesoporous particles, *etc.* [12–14].

Among these nanostructures, mesoporous semiconductors with microsphere-shape structure have been widely studied due to their excellent architecture properties, the existence of mesoporous not only is beneficial to produce advanced available surface area, which could provide more active sites to cause more surface

* Corresponding author. Tel.: +86 29 82663189.
** Corresponding author.
E-mail addresses: guidongyang@mail.xjtu.edu.cn (G. Yang), dingsj@mail.xjtu.edu.cn (S. Ding).

http://dx.doi.org/10.1016/j.apsusc.2014.05.060
0169-4332/© 2014 Elsevier B.V. All rights reserved.

Please cite this article in press as: T. Wang, et al., Orthogonal synthesis, structural characteristics, and enhanced visible-light photocatalysis of mesoporous Fe_2O_3/TiO_2 heterostructured microspheres, Appl. Surf. Sci. (2014), http://dx.doi.org/10.1016/j.apsusc.2014.05.060

absorbability of organic pollutant molecules, but also can contribute to develop mass transport through the materials [15]. On the other hand, the development of mesoporous semiconductor with microsphere-shape has been the focus of research due to their intrinsic shape-dependent characteristics, such as tunable pore structure, large surface area, high surface-to-volume ratios, uniquely optical, electronic and catalytic properties. Very recently, Xiang et al. [16] have synthesized 3D urchin-like hierarchical TiO_2 microspheres material by a simple solvothermal method without using any template or surfactant, and the obtained sample exhibits an excellent photocatalytic activity. Xiang et al. [17] reported the as-prepared Ag-TiO_2 nanocomposite hollow spheres show a high photodegradation of RhB under exposure of sunlight. Gao and Sun [18] found that the graphene-oxide/TiO_2 microsphere composites synthesized by the ultrasonic mixing of GO sheets with TiO_2 microspheres on the microscale also show the highly efficient hydrogen production.

However, a crucial drawback of TiO_2 microspheres is the relatively wide band gap (3.2 eV for anatase), which only can be excited by UV light (wavelength $\lambda < 387$ nm and the UV light accounts for about 4% of the solar energy on the Earth's surface), and therefore limits their practical applications [19]. Besides, titanium oxide generally suffers from a high recombination rate of photogenerated electrons and holes, consequently owns relatively low quantum efficiency [20], and which further limits its applications in solar-driven water purification [13,21–23]. In order to break through the limitations and utilize a larger portion of solar energy, especially enhance the photocatalytic activity of TiO_2 by irradiation under visible light, a growing number of studies have been explored. To date, several chemical methods have been used to modify TiO_2 properties, such as deposition of noble metals (Pt, Au, Ag) [24–26], doping of cations (Fe^{3+}, K^+, Na^+) [27,28] and anions (N, F) [29], and coupling with other semiconductors (CdS, ZnO, WO_3) [30]. Among these methods, the promising technique to harvest the most sunlight and enhance quantum yield of TiO_2 is coupling with a narrow band gap semiconductor to form heterojunction [31–34]. Very recently, the combination of Fe_2O_3 and TiO_2 as heterostructured materials has been extensively investigated because the Fe_2O_3 has the advantages of the matched band structure and requisite band energy for TiO_2 to form a valid heterojunction system [15,35]. Besides, the Fe_2O_3 has a narrower band gap (2.2 eV) [36], so electron–hole pairs in valence band of Fe_2O_3 is easier to be excited under visible light irradiation, and thus the formation of TiO_2/Fe_2O_3 composite could show wider visible-light-responsive range and stronger visible light absorption. More importantly, the formed junctions between Fe_2O_3 and TiO_2 in the composition system can promptly transfer electrons, avoiding the recombination of electron–hole pairs, and also supply more reaction active sites to improve the photocatalytic performance of the catalyst. Recently, Zhu et al. [37] fabricated 1D Fe_2O_3/TiO_2 tube-like nanostructures with quasi-single crystalline TiO_2 shells through a controllable way. The special core/shell nanostructures exhibited enhanced ethanol sensing properties with respect to the monocomponent.

Herein, an effective yet simple solvothermal method has been developed for the controlled synthesis of mesoporous Fe_2O_3/TiO_2 heterostructured microspheres. Meanwhile, orthogonal experimental design method was used to optimize the preparation conditions for the synthesis of mesoporous Fe_2O_3/TiO_2 heterostructured microspheres. Accordingly, several parameters, such as reaction temperature, amount of glucose and molar ratio of Fe to Ti, which significantly influence the photocatalytic properties, were investigated based on the orthogonal method. The obtained mesoporous Fe_2O_3/TiO_2 microspheres are characterized by thermogravimetry (TG), X-ray diffraction (XRD), scanning electron microscope (SEM), transmission electron microscopy (TEM), fourier transform infrared (FT-IR), UV–vis diffuse reflectance spectra (UV–vis DRS), and nitrogen adsorption/desorption. The photocatalytic performances of mesoporous Fe_2O_3/TiO_2 microsphere catalysts were measured by the photodegradation of RhB under visible light. Characterization results show that the as-prepared catalysts exhibit highly visible light photoactivity because of their mesoporous microsphere structure and high electron–hole separation efficiency.

2. Experimental

2.1. Synthesis

The mesoporous Fe_2O_3/TiO_2 heterostructured microspheres were synthesized via solvothermal method. The ferric chloride and tetrabutyl titanate were used as metal precursor salts and titanium source, respectively. Briefly, tetrabutyl titanate was dissolved into 20 mL of ethanol solution containing 3 mL of glacial acetic acid under vigorous stirring to form solution A, and the desired amount of glucose was dissolved into 8 mL of distilled water to form glucose solution B. Then, solution B was added dropwise into the solution A accompanying with continuously stirring at room temperature to form mixture solution. In succession, the desired amount of $FeCl_3$ was dissolved in the mixture under vigorous stirring until the clear khaki solution was achieved. The mixture was then transferred into a teflon-lined autoclave and heated under different reaction temperatures for 24 h, the heated suspension was removed from the oven and cooled to room temperature naturally. Afterwards, the suspension was filtrated and washed several times with deionized water and ethanol to remove impurities. The washed precipitate was dried at 80 °C overnight and then calcined at 400 °C for 4 h with a ramp rate of 1 °C/min in muffle furnace under stationary air to obtain the final heterostructured Fe_2O_3/TiO_2 microspheres. For comparison, pure TiO_2 and Fe_2O_3 microsphere samples were also synthesized using the similar processes, which only use tetrabutyl titanate (0.01 mol) and ferric chloride (0.01 mol) as starting materials, respectively (the added amounts of glucose is 3.4 g, and the reaction temperature is 140 °C).

In order to investigate the influence of the preparation conditions on the morphology, optical absorption, crystal structure and photocatalytic activities of mesoporous Fe_2O_3/TiO_2 heterostructured microspheres, three synthesis parameters: reaction temperature, amount of glucose and Fe:Ti molar ratio were chosen as the most important factors to design the preparation experiments, and the corresponding factors and their levels are shown in Table S1. According to the synthesis conditions and parameters, a L_9 orthogonal array contained nine rows and four columns were chosen and the results list in Table S2. It can be seen the whole preparation experiments requires nine test for the synthesis of Fe_2O_3/TiO_2 heterostructured microspheres, and thus the optimal preparation conditions can be obtained from the a minimum possible number of experiment. The as-prepared photocatalysts were denoted as FT-1, FT-2, FT-3, FT-4, FT-5, FT-6, FT-7, FT-8 and FT-9, respectively.

2.2. Characterization

Thermogravimetric analysis (Perkin-Elmer TGA 7) was collected under a flow of employed air at temperature ramp of 20 °C/min from room temperature to 1000 °C. The crystalline structure and phase component were obtained on powder X-ray diffraction (XRD; SHIMADZU, Lab X XRD-6000). The scanning electron microscopy (SEM) images were obtained with field-emission scanning electron microscope (JEOL, JSM-6700F) to obtain the geometry and morphology of the Fe_2O_3/TiO_2 microspheres. Energy dispersive X-ray spectroscopy (EDX) was also employed for elemental

Please cite this article in press as: T. Wang, et al., Orthogonal synthesis, structural characteristics, and enhanced visible-light photocatalysis of mesoporous Fe_2O_3/TiO_2 heterostructured microspheres, Appl. Surf. Sci. (2014), http://dx.doi.org/10.1016/j.apsusc.2014.05.060

analysis. Transmission electron microscopy (JEOL, JEM-2100) was used to observe the structure and surface state of photocatalyst composites. Diffuse reflectance UV–vis diffuse reflectance spectra (DRS) were measured on a Hitachi U-4100 instrument employed with a lab-sphere diffuse reflectance accessory. Fourier transform infrared (FT-IR) spectra were carried out on Nicolet avatar 360 FT-IR by potassium bromide tablet method. Nitrogen adsorption–desorption isotherms were collected at liquid nitrogen temperature on an ASAP3000 apparatus, the samples were degassed at 120 °C for 2 h before the actual measurement. Pore-size distributions were counted by the Barrett–Joiner–Halenda (BJH) model with Halsey equation using the desorption branch of the absorption isotherms and surface areas were calculated using Brunauer–Emmett–Teller (BET) method.

2.3. Photocatalytic test

The photocatalytic activities of all the mesoporous Fe_2O_3/TiO_2 heterostructured microspheres were evaluated by decomposing rhodamine B (RhB) dye under visible light irradiation at room temperature. The photocatalytic reaction system consisted of an overhead 300 W Xenon lamp (HSX-F300, Beijing NBeT) equipped with UV filter (HSX-UV300) and placed above the RhB solution with a distance of about 10 cm, which were mounted a 420 nm cut-off glass filter and all UV light were completely removed in order to ensure only visible light irradiation. In each experiment, reaction suspension was prepared by adding 0.07 g photocatalyst into 70 mL aqueous solution of RhB dye solution (10 mg/L). The suspension was then magnetically stirred in dark for 40 min to establish an adsorption/desorption equilibrium between the catalyst and the RhB solution, then the solution was exposed to the visible light and the degradation reaction was occurred. During photoreaction, the suspension (about 3 mL) was taken from the reactor at regular intervals and centrifuged (13,000 rpm for 5 min) to remove the photocatalysts, and the concentration of the remaining RhB solution was analyzed by UV–vis spectrophotometer (UV-1900PPC, Shanghai, China), and the characteristic absorption peak of RhB at 554 nm was used to determine the degradation efficiency (x) of RhB, which can be calculated by the following formulation:

$$x = \frac{C}{C_o} \times 100\%$$

where C_o is the original concentration of RhB when the solution reached to adsorption/desorption equilibrium, C is the residual concentration of RhB solution after each photoreaction.

3. Results and discussion

3.1. The optimum synthesis parameters

In order to maximize the photocatalytic performance of mesoporous Fe_2O_3/TiO_2 microspheres, nine samples were prepared according to L_9 orthogonal array listed in Table S3 (supporting information). The performance of each sample towards RhB degradation reaction was considered as response data, and the corresponding degradation efficiencies (within 150 min photoreaction) of all the samples are also shown in Table S3. Herein, the signal-to-noise ratio of the response data was used to measure the quality characteristic deviation from the desired value, and the main effects plot for the means of signal-to-noise ratio was shown in Fig. S1. In fact, main effects plot shows how each factor specifically affects the response, and which also indicates the general trend of the influence of the factors. By comparing the slopes of the lines, we can estimate the relative magnitude of the effects. Moreover, the optimum condition also can be identified by studying the main effects of each factor [38]. Table S4 shows the signal to noise ratio response table for the photocatalytic activity of Fe_2O_3/TiO_2 microspheres, and the means of signal to noise ratio for each level of the factors are also summarized in Table S4. It can be found that reaction temperature is the most important parameter affecting the photocatalytic activity. As is well known, the optimum reaction temperature contributes to the improvement of the crystallization of Fe_2O_3/TiO_2 microspheres. Consequently, the separation of photogenerated electron–hole pairs can be increased with the higher crystallization. The effect factor is followed by the amount of glucose. Glucose molecules play a vital role in the preparation process because the amount of glucose could influence the sample's morphology and structure, as a result of affecting the photocatalytic performance. The last effect factor is the molar ratio of Fe to Ti, which affects the component of Fe_2O_3 and TiO_2 in the obtained microspheres. In general, the larger the signal-to-noise ratio, the higher contribution of one effect factor at that level for the photocatalytic activity of Fe_2O_3/TiO_2 microspheres. Therefore, as shown in Table S4, the optimum preparation conditions for the synthesis of mesoporous Fe_2O_3/TiO_2 heterostructured microspheres can be found to be reaction temperature at 140 °C, the amount of glucose of 3.4 g and the Fe:Ti molar ratio of 0.005:0.01, and the optimum preparation conditions is completely consistent with the synthesis of FT-1 sample. As can be seen from Table S3, the degradation rate of FT-1 under visible light irradiation is high even up to 97% within 150 min photoreaction.

3.2. Characteristic analysis of mesoporous Fe_2O_3/TiO_2 microspheres

The thermogravimetric (TG) and differential thermal analysis (DTA) of FT-1 are depicted in Fig. 1. The TG curve of mesoporous Fe_2O_3/TiO_2 heterostructured microspheres shows three weight-loss stages. As shown, the first event occurred in the region of 25–100 °C, which probably involved in desorption of physically adsorbed water and ethanol on the catalysts surface. This process was also confirmed by the appearance of the endothermic peak at ~50 °C on the DTA trace. The second and third events occurred between the temperature ranges of calcination temperature at 100–230 °C and 230–400 °C, respectively. While DTA curve showed two exothermic peaks in these ranges: one at 280 °C and another at 380 °C. As discussed previously, the two peaks may be due to the decomposition of unhydrolyzed Ti precursor remained in the TiO_2 xerogel powders, as well as the degradation and burning of glucose molecules. Therefore, the suitable calcinations temperature was chosen at 400 °C.

Powder X-ray diffraction (XRD) in the range of $2\theta = 10 \sim 80°$ was used to evaluate the phase structure and crystallite size of the

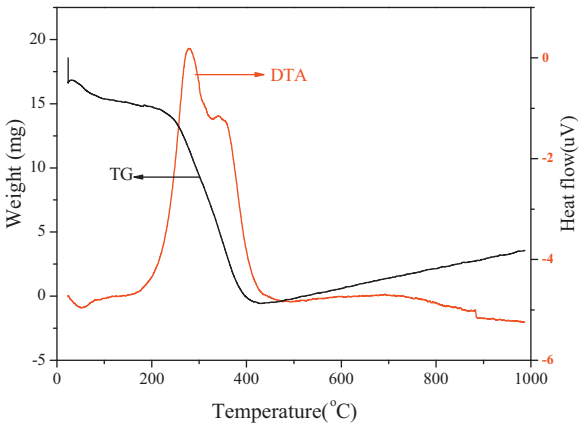

Fig. 1. TG and DTA curves of FT-1.

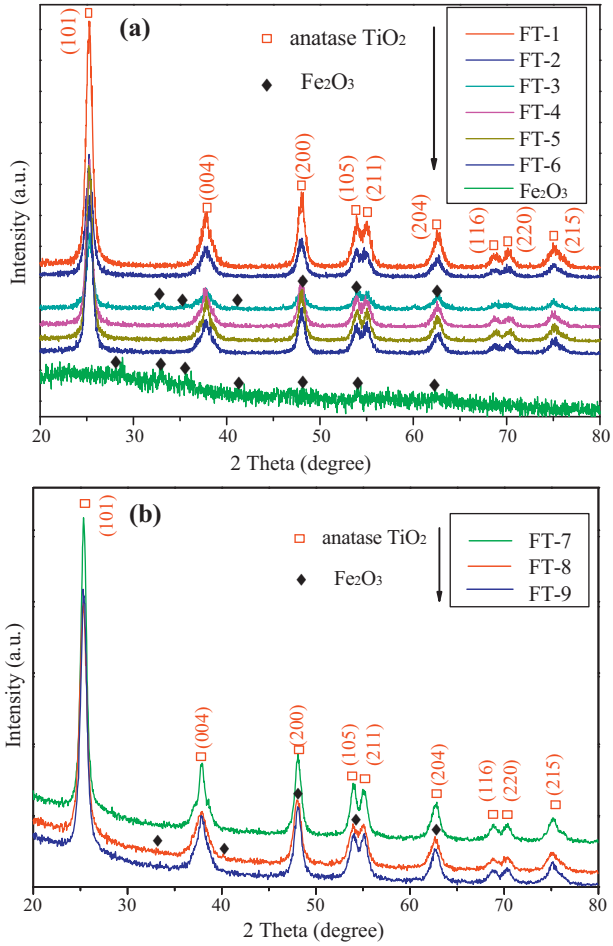

Fig. 2. XRD patterns of all mesoporous Fe_2O_3/TiO_2 heterostructured microspheres (a) FT-1, FT-2, FT-3, FT-4, FT-5, FT-6, pure Fe_2O_3; (b) FT-7, FT-8, FT-9.

as-prepared photocatalysts. Fig. 2 shows the XRD patterns of all the mesoporous Fe_2O_3/TiO_2 heterostructured microspheres, including data for pure Fe_2O_3 microsphere sample, used here as a reference. As shown, the diffraction peaks at 33.15°, 35.61°, 40.85°, 48.13°, 54.05° and 62.65° in the XRD pattern of pure Fe_2O_3 can be attributed to the (1 0 4), (1 1 0), (1 1 3), (0 2 4), (1 1 6) and (2 1 4) crystal planes of hematite Fe_2O_3 (JCPDS: 33-0664). Meanwhile, a relatively low diffraction intensity of Fe_2O_3 microsphere can be observed, indicative of a lower crystallinity for the sample. Additionally, all the mesoporous Fe_2O_3/TiO_2 microsphere samples (except FT-3 and FT-8 sample) indicate similar XRD curve, several peaks can be observed at the position of 25.26°, 37.93°, 48.13°, 53.91°, 54.09°, 62.45°, 68.82°, 70.12° and 75.43° in the XRD patterns of Fe_2O_3/TiO_2 microspheres, which can be indexed to the (1 0 1), (0 0 4), (2 0 0), (1 0 5), (2 1 1), (2 0 4), (1 1 6), (2 2 0) and (2 1 5) planes of anatase TiO_2 crystal (JCPDS: 21-1272). No characteristic peaks for Fe_2O_3 were found in these samples, suggesting that only a small quantity of Fe_2O_3 nanoparticles is attached on the TiO_2 to form the heterostructured microspheres, and which is either highly dispersed or under the detection limit of XRD. However, it should be noted that the diffraction peaks related to the iron oxide can be clearly observed in FT-3 and FT-8 sample, indicating that the co-existence of Fe_2O_3 and TiO_2 in the composites. In addition, it can be observed that the main Bragg diffractions of all the samples are very sharp and intense after the solvothermal reaction, indicating that these samples have high crystallinity, which might be favorable for the enchantment of photocatalytic activity under visible light irradiation.

Furthermore, the average crystallite size of all the Fe_2O_3/TiO_2 microspheres was calculated using Scherrer's formula: $D = K\lambda/\beta\cos\theta$ [39], where D is the crystallite size, λ is the wavelength of X-ray radiation (0.154 nm), β is the full width of (1 0 1) plane of TiO_2 at half-maximum, θ is the diffraction angle, and K is usually taken as 0.89. The calculated results of all samples' crystallite size of TiO_2 are shown in Table 1. It can be seen that the average crystallite size of mesoporous Fe_2O_3/TiO_2 heterostructured microspheres is centralized in the range of 9.5 ~ 13 nm.

Fig. 3 shows the typical SEM images of all the as-prepared mesoporous Fe_2O_3/TiO_2 microspheres as well as the pure Fe_2O_3 and pure TiO_2 reference sample. As shown, no noticeable changes have been found for these composite photocatalysts, and all of the mesoporous Fe_2O_3/TiO_2 samples including the pure Fe_2O_3 sample possess a well-defined micro-spherical structure with average particles size of 0.6 ~ 1 μm, indicating that the method is a very useful technique to synthesize the Fe_2O_3/TiO_2 microspheres with mesoporous structures. In Fig. 3(c), the image of pure TiO_2 reveals presence of some agglomerates or aggregations which consisted of some nanoparticles and nanospheres with 100 ~ 150 nm in diameter. Furthermore, the individual Fe_2O_3/TiO_2 particles showed in the inset of Fig. 3(d) and (e) also confirm that the obtained photocatalysts have representative spherical structures. Interestingly, the magnified SEM image of FT-7 depicted in Fig. 3(j) reveals that the formation of Fe_2O_3/TiO_2 microspheres were composed of many tiny nanocrystals with size of ~10 nm, which is in good agreement with the average crystal size of the catalysts calculated by XRD analysis. Meanwhile, a rough surface for Fe_2O_3/TiO_2 microspheres can be distinctly observed, this may be attributed to the Fe_2O_3 nanoparticles accumulate on the TiO_2 surface and contribute a large surface area and more active centers on the surface of the micro-spherical photocatalysts, as a result of leading to a high photocatalytic performance. As clearly depicted in the SEM images of all the samples, porosity is evident in the aggregation, which may offer transport paths for organic pollutant molecules and promoted photocatalytic performance. Fig. 3(a) shows the energy dispersive X-ray spectrum (EDX) of FT-1 sample, it can be seen that the micro-spherical catalyst contained Fe, Ti, O elements (the atomic percentage of Fe, Ti and O are 0.24, 5.01 and 21.83, respectively), suggesting that the presence of Fe and O elements on the surface of TiO_2 and form a

Table 1
BET surface area, pore volume, pore diameter, average crystallite size and atomic ratio of Ti to Fe of all the prepared catalysts.

Catalyst	S_{BET} (m^2/g)	Pore volume (cm^3/g)	Pore size (nm)	Crystallite size (nm)	Ti:Fe atomic ratio
FT-1	97.25	0.21	8.73	10.10	20.8:1
FT-2	112.7	0.43	15.16	10.33	25.4:1
FT-3	112.02	0.33	11.62	11.58	3:1
FT-4	144.2	0.41	11.24	10.10	25.8:1
FT-5	131.2	0.41	12.37	12.72	25.0:1
FT-6	91.5	0.15	6.72	9.47	37.1:1
FT-7	123.0	0.51	16.68	12.11	10.5:1
FT-8	80.2	0.13	12.42	10.25	31.8:1
FT-9	114.3	0.32	11.38	10.10	23:1

Please cite this article in press as: T. Wang, et al., Orthogonal synthesis, structural characteristics, and enhanced visible-light photocatalysis of mesoporous Fe_2O_3/TiO_2 heterostructured microspheres, Appl. Surf. Sci. (2014), http://dx.doi.org/10.1016/j.apsusc.2014.05.060

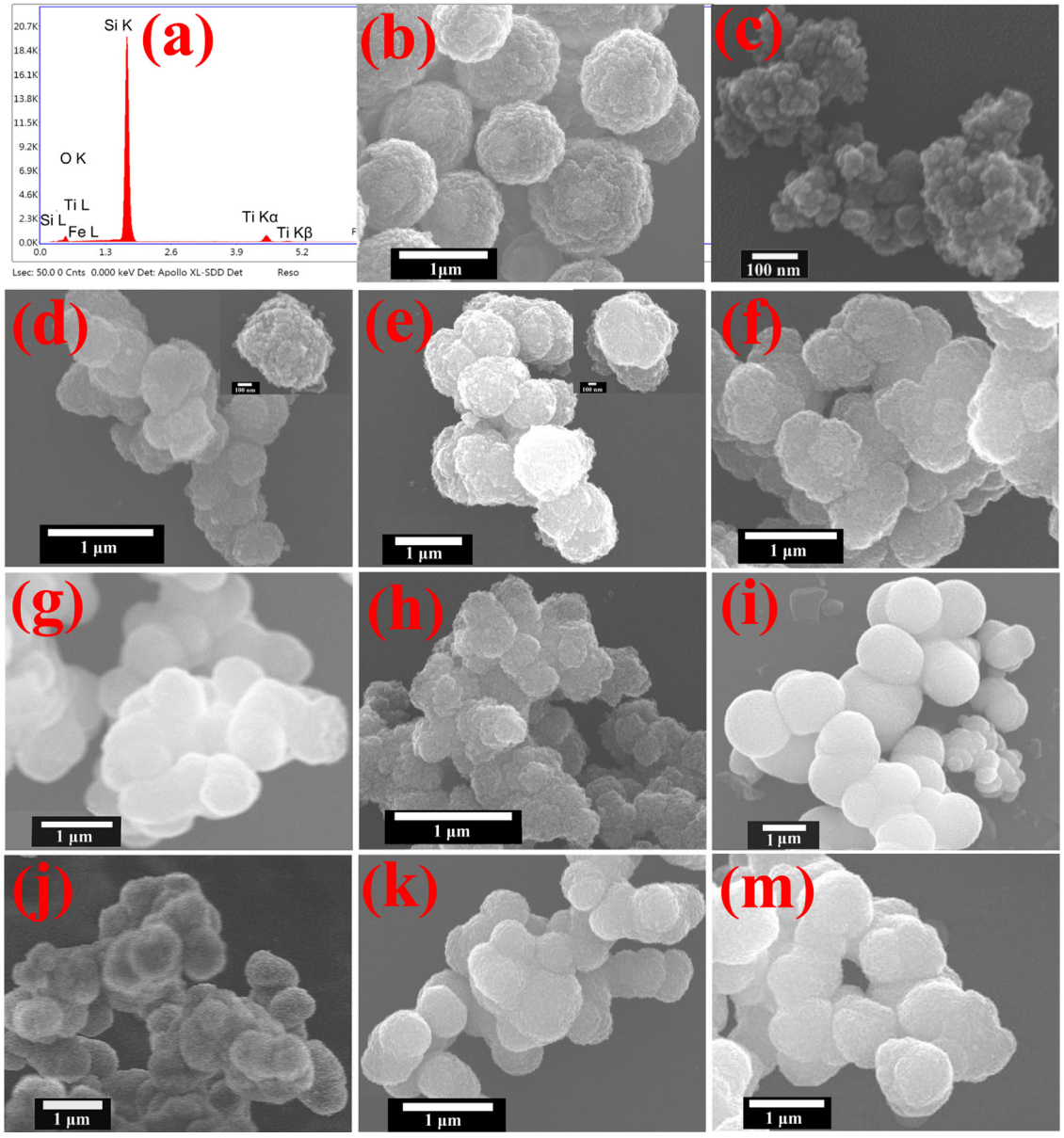

Fig. 3. (a) Energy dispersive X-ray spectrum of FT-1; SEM images of (b) pure Fe_2O_3; (c) pure TiO_2; (d) FT-1 (inset is the individual microsphere of FT-1); (e) FT-2 (inset is the individual microsphere of FT-2); (f) FT-3; (g) FT-4; (h) FT-5; (i) FT-6; (j) FT-7; (k) FT-8; (m) FT-9.

continuous phase of Fe_2O_3. By the way, the strong peak of Si element (atomic percentage of 72.91) was also observed in the spectrum, this can attributed to the utilization of the silicon substrate in the SEM testing process. In addition, the elemental compositions of the rest of mesoporous Fe_2O_3/TiO_2 heterojunctions (from FT-2 to FT-9 samples) were also monitored using the EDX analysis, and the corresponding EDX spectra of these samples were shown in Fig. S2. Based on the EDX results, the atomic molar ratios of Fe to Ti in each sample were calculated and summarized in Table 1.

The typical TEM image of the FT-1 sample was shown in Fig. 4. As shown in Fig. 4(a) and (b), the Fe_2O_3/TiO_2 heterojunctions consist of uniform microspheres with an average diameter of about 700 nm, and these microspheres with a relatively rough surface are composed of a large quantity of nanoparticles with an average particles size of 10 nm. The above analytical results are consistent with the SEM analysis. As shown in Fig. 4(c) (HR-TEM image of FT-1 sample), the lattice fringes of the nanocomposite material can be observed clearly, which proves the good crystallinity of mesoporous Fe_2O_3/TiO_2 microspheres. In addition, the reflection with *d* spacing values of 0.207 nm and 0.238 nm observed in Fig. 4(c) can be well indexed to the Fe_2O_3 crystal (2 0 2) lattice plane and TiO_2 crystal (0 0 4) lattice planes, respectively, indicating that the formation of TiO_2 phase with the co-existence of a small amount of Fe_2O_3 and thus a distinct juncture can be naturally formed in the composite system. From the selected area electron diffraction (SAED) pattern invested on FT-1 (Fig. 4(d)), a sequence of diffraction rings can be clearly found, indicating that the whole spherical particles have a "poly-crystalline aggregates" structure and further confirming that the Fe_2O_3/TiO_2 heterostructured microsphere has highly crystallized feature, in good agreement with the HR-TEM image.

Fig. 5 shows the nitrogen adsorption/desorption isotherms and the corresponding pore size distribution curves of the mesoporous Fe_2O_3/TiO_2 microspheres. The adsorption isotherms (Fig. 5(a)) of all the samples show typical IV isotherm according to the IUPAC classification, illustrating a clear characteristic of mesoporous structure of solid. Additionally, the adsorption hysteresis loop of the isotherm

Please cite this article in press as: T. Wang, et al., Orthogonal synthesis, structural characteristics, and enhanced visible-light photocatalysis of mesoporous Fe_2O_3/TiO_2 heterostructured microspheres, Appl. Surf. Sci. (2014), http://dx.doi.org/10.1016/j.apsusc.2014.05.060

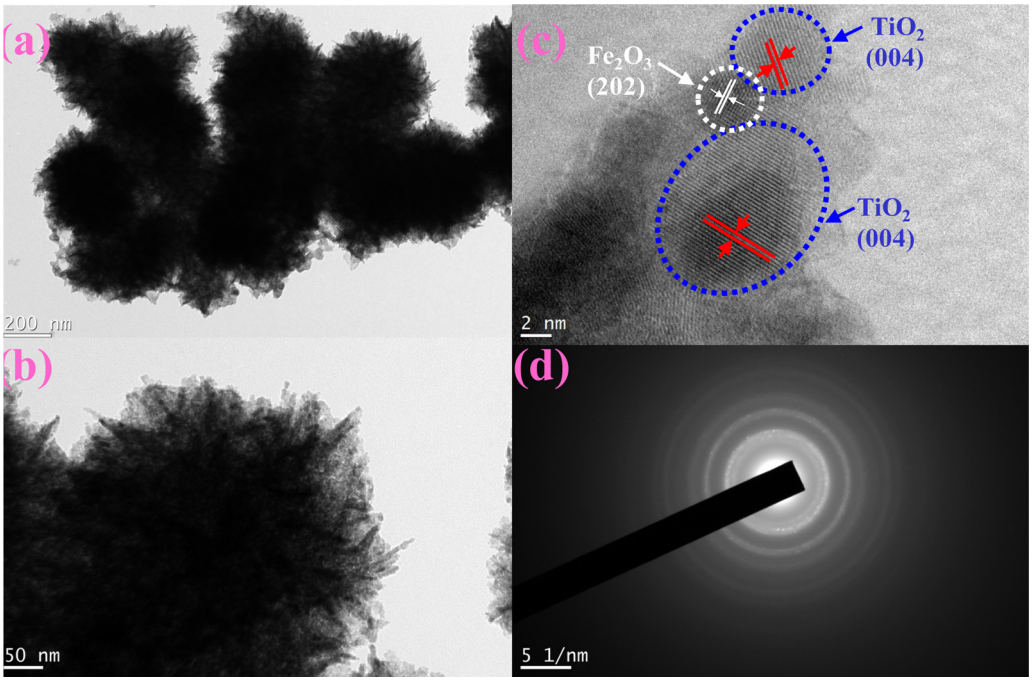

Fig. 4. TEM image of FT-1 (a, b); HR-TEM image of FT-1 (c); selected-area electron diffraction pattern of FT-1 (d).

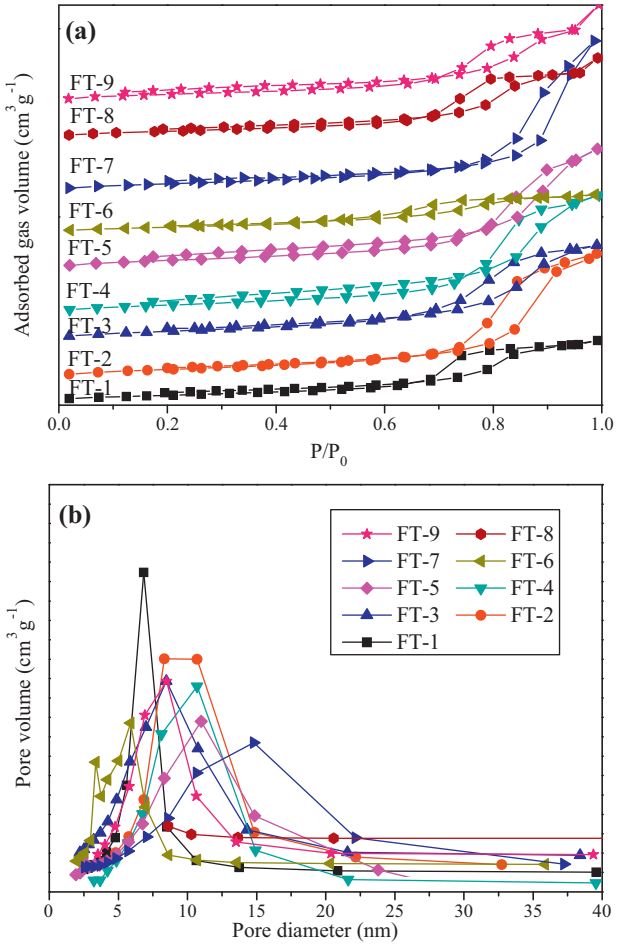

Fig. 5. (a) N_2 adsorption–desorption isotherms of mesoporous Fe_2O_3/TiO_2 heterostructured microspheres; (b) corresponding pore size distribution of mesoporous Fe_2O_3/TiO_2 heterostructured microspheres.

can be assigned to the type-B, indicating that the presence of slit-like pores in the surface of the mesoporous Fe_2O_3/TiO_2 microspheres, this is consistent with SEM analysis. As shown in Fig. 5(b), the pore size distribution calculated by the BJH method based on the desorption branch of all the samples showed similar narrow pore size distributions. Among these samples, FT-1 and FT-6 show a relative smaller mesopores, which are centered at 3.5 ~ 6.7 nm, whereas others show the relatively larger mesopores with wide pore size distribution of 8 ~ 17 nm range. Based on the above-mentioned results, it can be clearly concluded that the as-prepared Fe_2O_3/TiO_2 microsphere samples have an obvious mesoporous structure, which may be arose from the organized aggregation of Fe_2O_3 and TiO_2 nanoparticles that formed by weak coordination interactions during the solvothermal process.

Moreover, the BET surface area and average pore size of all Fe_2O_3/TiO_2 microspheres are summarized in Table 1. It can be seen that the as-prepared catalysts have high surface area centered in the range of 80.2 ~ 144.2 m^2/g, which can be attributed to the preservation of mesoporous structure in the Fe_2O_3/TiO_2 microspheres.

Fig. 6 shows the FT-IR spectra of all the mesoporous Fe_2O_3/TiO_2 catalysts synthesized by solvothermal method, which can provide the information of functional groups on the surface of materials. The broad peak at around 3400 cm^{-1} and 1630 cm^{-1} can be assigned to the stretching vibration of absorbed water molecules and the bending vibration of hydroxyl group existed on the oxide surface, respectively [40,41]. As is known to all, these functional ^-OH groups play a vital role in photocatalytic degradation process since they can react with photoexcited holes and form hydroxyl radical, which could act as an active oxidizer to result in the decomposition of organic pollutants [42]. In addition, a remarkable wide band ranging from 480 cm^{-1} to 800 cm^{-1} is detected in the FT-IR spectra of all the samples, which can be assigned to the overlapping peak between the Ti–O–Ti bridging stretching modes and Fe–O vibrations [9,43,44], indicating that the co-existence of Fe_2O_3 and TiO_2 phase in the mesoporous Fe_2O_3/TiO_2 hereojunction microspheres.

Fig. 7 shows the UV–vis diffuse reflectance spectra of all the mesoporous Fe_2O_3/TiO_2 microsphere samples. It is clear that pure

Please cite this article in press as: T. Wang, et al., Orthogonal synthesis, structural characteristics, and enhanced visible-light photocatalysis of mesoporous Fe_2O_3/TiO_2 heterostructured microspheres, Appl. Surf. Sci. (2014), http://dx.doi.org/10.1016/j.apsusc.2014.05.060

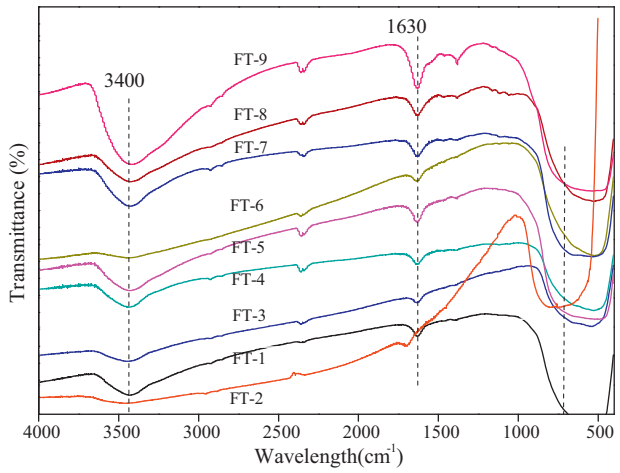

Fig. 6. FT-IR spectra of pure TiO_2 and all the as-prepared mesoporous Fe_2O_3/TiO_2 heterostructured microspheres.

TiO_2 show no adsorption in visible light region owing to its wide band gap (3.2 eV). In comparison with pure TiO_2, all the heterostructured Fe_2O_3/TiO_2 samples exhibit an apparent optical absorptivity in the visible light range between 390 and 550 nm. As well know, Fe_2O_3 is one of narrow energy band gap (2.2 eV) semiconductors and shows stronger visible light absorption. Thus, it is believed that the expansion of the adsorption edge of the mesoporous Fe_2O_3/TiO_2 microspheres is resulted from the photosensitization of Fe_2O_3. Moreover, the formation of heterojunctions through the incorporating Fe_2O_3 with TiO_2 could alter the electronic structure of microsphere photocatalysts and promote the separation of photogenerated electron–hole pairs, as result of leading to the enhancement of the photocatalytic performance of catalysts under visible light irradiation.

In order to evaluate the photocatalytic activity of all the samples, the RhB dye was chosen as the target pollution due to its higher stability. Fig. 8(a) depicts the absorption spectra variation of RhB versus visible light irradiation time in presence of the optimized Fe_2O_3/TiO_2 sample (FT-1). As shown, FT-1 sample shows quite high photocatalytic activity and the characteristic absorption band of RhB at 554 nm diminished quickly with a slight accompanying blue-shift from 554 nm to 490 nm of the maximum absorption band, suggesting that RhB solution has been completely decomposed and mineralized in the Fe_2O_3/TiO_2 microspheres environment.

Fig. 8(b) shows the visible light induced photocatalytic activity for the degradation of RhB over all the mesoporous Fe_2O_3/TiO_2 heterostructured microspheres obtained by different preparation conditions, pure Fe_2O_3 and pure TiO_2 microspheres. It can be seen that the direct illumination without catalyst as the blank control could lead to only about 2% decomposition of RhB solution within 240 min, which accounts for the photosensitized capability of RhB molecules. As expected, the pure TiO_2 show no photocatalytic activity under visible light irradiation, because it could not be activated by visible light due to its wide energy gap (3.2 eV) [45]. However, it is interesting that the pure Fe_2O_3 also show no photocatalytic activity for degradation RhB solution, this phenomenon can be explained by the following reasons: on the one hand, although the Fe_2O_3 with narrow band gap can be excited to generate electron–hole pairs on the surface of catalyst, due to the quite lower charge separation efficiency, most of charges quickly recombine without doing any photochemistry reaction [46]. On the other hand, the XRD data show the pure Fe_2O_3 microsphere has a lower crystalline degree, which is unfavorable for the transfer of photoelectron from bulk to surface and thus restrain a large number of electrons to participate in photocatalytic reaction, resulting in low reactivity. In contrast, all the mesoporous Fe_2O_3/TiO_2 microspheres showed much higher photocatalytic activities than the reference samples under visible light irradiation, suggesting that an efficient charge separation occurred in the junctions between Fe_2O_3 and TiO_2,

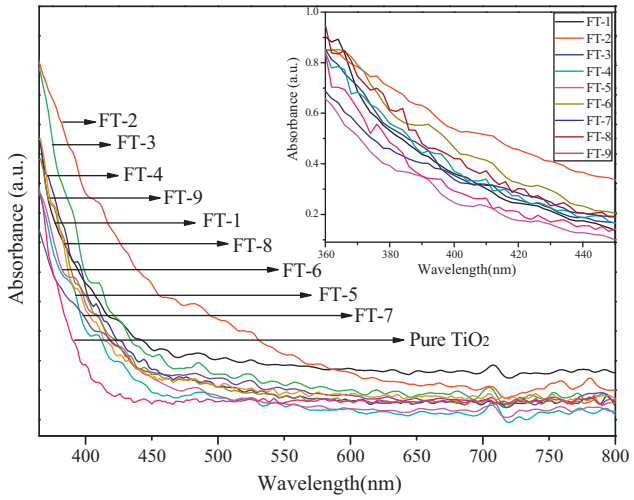

Fig. 7. UV–vis diffuse reflectance spectra of mesoporous Fe_2O_3/TiO_2 heterostructured microspheres. The inset is the enlarged localized profiles of the samples.

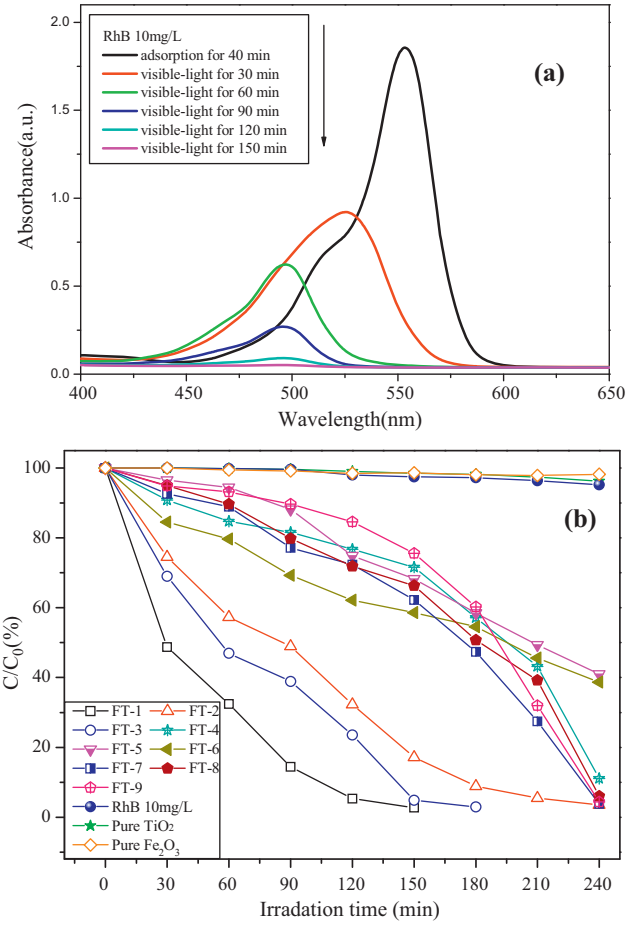

Fig. 8. (a) UV–vis absorbance spectra changes of RhB as a function of photoreaction time in presence of FT-1; (b) photocatalytic degradation of RhB over all the as-prepared Fe_2O_3/TiO_2 heterostructured microspheres, pure TiO_2, pure Fe_2O_3 and no catalyst under visible-light irradiation.

Please cite this article in press as: T. Wang, et al., Orthogonal synthesis, structural characteristics, and enhanced visible-light photocatalysis of mesoporous Fe_2O_3/TiO_2 heterostructured microspheres, Appl. Surf. Sci. (2014), http://dx.doi.org/10.1016/j.apsusc.2014.05.060

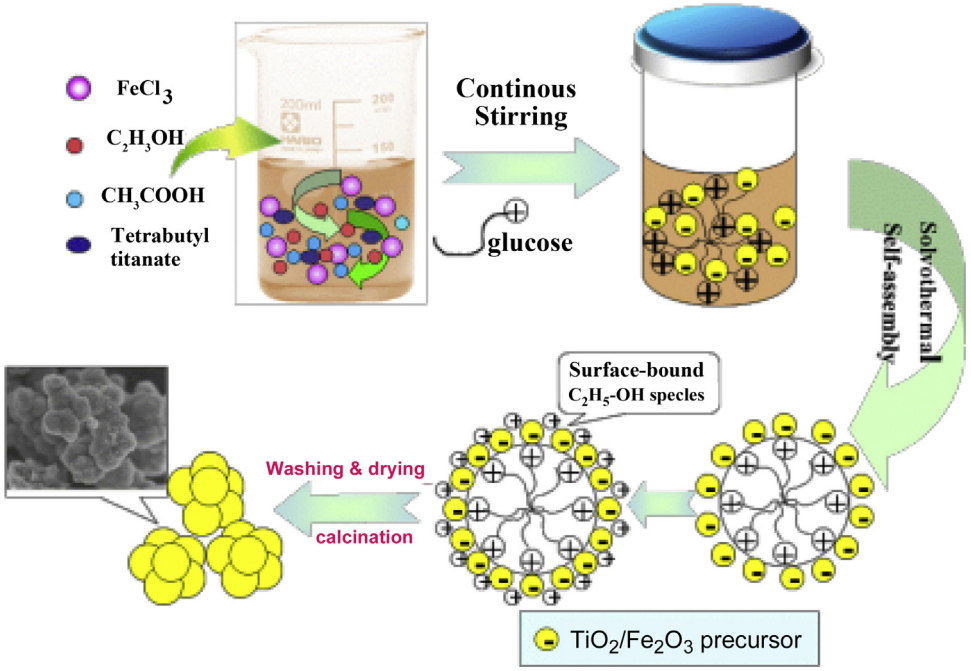

Fig. 9. Schematic diagram for the fabrication of mesoporous Fe_2O_3/TiO_2 heterostructured microspheres.

and thus increased the life time of the charge carriers to perform photodegradation reaction. Among these samples, FT-1 shows the highest photodegradation performance, and the degradation rate of RhB solution reaches about 94.7% within 120 min photoreaction. Next, the FT-3 and FT-2 show relatively higher catalytic performance for the decomposition of RhB, and the degradation rates are about 76.45% for FT-3 and 67.68% for FT-2, respectively, in the same irradiation time. Moreover, the rest of samples show lower catalytic performance, and their degradation yield is less than 40% within 120 min visible light photoreaction. In short, the order of photocatalytic activity is FT-1 > FT-3 > FT-2 > FT-7 > FT-9 > FT-8 > FT-4 > FT-6 > FT-5. So, it can be concluded that the varying preparation conditions have significant influence on the photocatalytic behavior of the Fe_2O_3/TiO_2 microspheres.

3.3. Formation mechanism of the Fe_2O_3/TiO_2 microspheres

Based on the above analysis and discussions, a possible formation mechanism of the mesoporous Fe_2O_3/TiO_2 heterostructured microspheres was proposed with the purpose of guiding the improvement of the photocatalytic performance. Fig. 9 shows the schematic diagram for the formation mechanism of the Fe_2O_3/TiO_2 microspheres. As previously reported [13], when the glacial acetic acid was introduced into the reaction system, the hydrolysis process of $Ti(OBu)_4$ can be efficaciously stabilized and restricted, while some $[Ti(OBu)_{4-n}(CH_3COO)_n]$ precursor as well as the $[FeCl_{3-n}(CH_3COO)_n]$ precursor generated rapidly in acidic conditions. On the other hand, the glucose molecules can self-assemble through hydrogen bonding to yield round globules during the initial solvothermal stage. Afterwards, the formed round globules of glucose quickly react with these small amorphous $[Ti(OBu)_{4-n}(CH_3COO)_n]$ nanoparticles and $[FeCl_{3-n}(CH_3COO)_n]$ nanoparticles, and thus form the $[Ti(OBu)_{4-n}(CH_3COO)_n(acid)(glucose)]$ and $[FeCl_{3-n}(CH_3COO)_n(acid)(glucose)]$ particles by weak coordination interactions and hydrogen bonding. During the continuously reaction, glucose molecules spontaneously aggregates into spheres to minimize the free energy of the system, while the highly reactive temperature drives the $[Ti(OBu)_{4-n}(CH_3COO)_n(acid)(glucose)]$ and $[FeCl_{3-n}(CH_3COO)_n(acid)(glucose)]$ species to react with oxygen and instantly self-assemble to generate an incompact Fe_2O_3/TiO_2 precursor nanoparticles on the surface of glucose globules. Meanwhile, the presence of surface-bound C_2H_5-OH species on exterior of spherical structure could provide a support for the framework of mesoporous structure, and thus favor the formation of final heterostructure of Fe_2O_3/TiO_2. With the reaction proceeds, the glucose cores can easily dehydrate water and thus transform glucose to carbonaceous species. At last, after washing and calcinations, the C_2H_5-OH and carbonaceous species can be easily removed, and eventually leading to the formation of mesoporous Fe_2O_3/TiO_2 microspheres.

3.4. Mechanism of charge separation and enhanced visible-light-driven activity

In this paper, we synthesized mesoporous Fe_2O_3/TiO_2 microspheres and the obtained photocatalysts show enhanced visible light activity for degradation of dyes, indicating that the samples might have potential applications in the cleanup of environment. Fig. 10 shows the schematic illustration of the electron transfer for the degradation of RhB over mesoporous Fe_2O_3/TiO_2 microspheres. As shown, when Fe_2O_3/TiO_2 microspheres and RhB reaction system is illuminated with visible light, the RhB dye molecules are firstly excited and generated photoelectrons (e^-), and subsequently the excited RhB* will inject electrons into the conduction band (CB) of TiO_2 [47–49]. Because of different band gap between Fe_2O_3 and TiO_2, the injected electrons in the CB of TiO_2 tend to transfer to the CB of Fe_2O_3 driven by the potential energy. Besides the self-sensitization of RhB molecules, the coupled Fe_2O_3 nanoparticles with narrow band gap of 2.2 eV also can be excited under visible light irradiation and produce electrons (e^-) and holes (h^+) pairs. The electrons have high reduction properties and rapidly diffuse to the CB of Fe_2O_3, while the same amounts of holes were still left in the VB. As demonstrated above, such charge carriers transfer in heterojunction system could effectively separate electron–hole (e^-–h^+) pairs and successfully inhibit their unfavorable recombination; therefore, this process prolongs life time of these charge carriers, as a result of leading to the increased quantum efficiency.

Please cite this article in press as: T. Wang, et al., Orthogonal synthesis, structural characteristics, and enhanced visible-light photocatalysis of mesoporous Fe_2O_3/TiO_2 heterostructured microspheres, Appl. Surf. Sci. (2014), http://dx.doi.org/10.1016/j.apsusc.2014.05.060

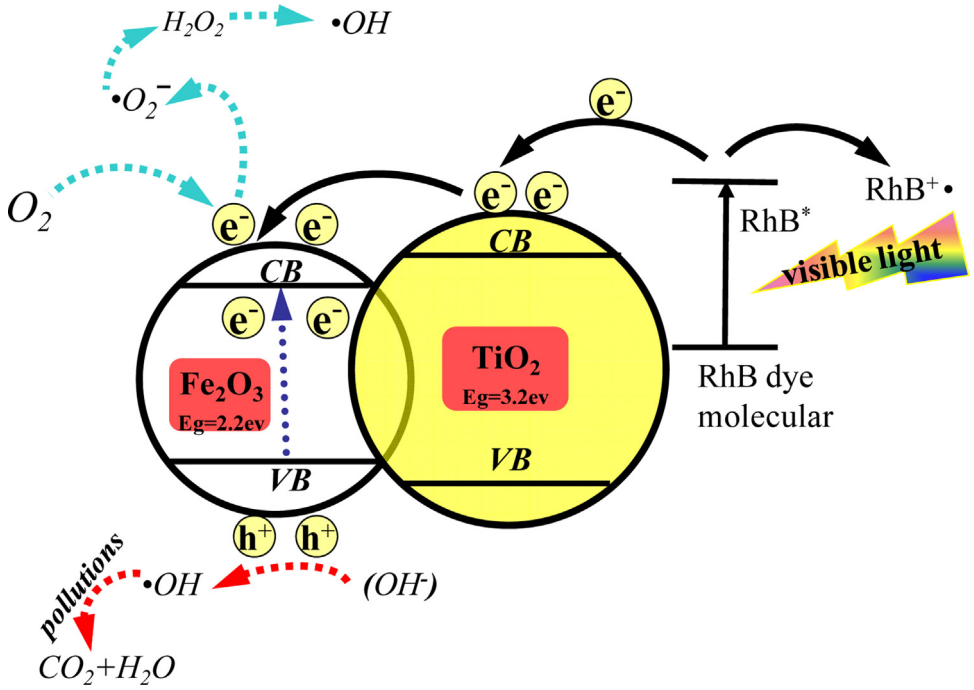

Fig. 10. The schematic illustration of the electron transfer mechanism for the degradation of RhB dye over mesoporous Fe_2O_3/TiO_2 heterostructured microspheres under visible light irradiation.

From the photoelectrochemistry point of view, the existent of electrons in the CB of Fe_2O_3 can be scavenged by the molecular oxygen present in water to generate superoxide radical ($O_2^{\bullet-}$) and hydrogen peroxide radical (H_2O_2), while the highly oxidative holes located on VB of Fe_2O_3 not only react with RhB molecules but also can oxidize water molecules to produce hydroxyl radicals ($^{\bullet}OH$). Both of them are response for the photodegradation of RhB dye.

Besides the characteristic heterostructure of Fe_2O_3/TiO_2 microsphere, the higher photocatalytic performance of Fe_2O_3/TiO_2 microspheres is also relied on their well crystallinity, larger specific surface area, uniform morphology and higher visible light absorption. Firstly, the XRD pattern shows these microspheres have well crystallized structure, which facilitate to promote the transfer of photoelectron from bulk to surface, and thus enhance the separation of charges, resulting in the enhancement of the quantum efficiency. Secondly, the mesoporous microsphere structure composed of many tiny nanoparticles can offer larger specific surface area and higher pore volume for the as-prepared photocatalysts, of which have been discussed in the BET section. It is well known that Fe_2O_3/TiO_2 microsphere with larger surface area and higher pore volume not only could provide more adsorption sites and surface active centers for better surface absorbability towards the target pollution but also have the merits for improving mass transfer of the reactant molecules, and both of them could contribute to the enhancement of photocatalytic activity. On the other hand, the Fe_2O_3/TiO_2 samples with higher specific surface area can further absorb more incident photons in photocatalytic process, which may favor the increase of light adsorption efficiency and excite more electron–hole pairs in the active sites. Thirdly, the coupled Fe_2O_3 can efficiently absorb visible light due to its low energy gap. Hence, when Fe_2O_3 attached on the TiO_2 nanoparticles and formed the heterojunction structure between the two individual components, the microsphere catalysts would result in an obviously visible light photocatalytic activity. As a consequence, we can attempt to conclude that the Fe_2O_3/TiO_2 microspheres show an excellent photocatalytic activity under visible light irradiation owing to the synergistic effect of their special microsphere structure, large surface area, high crystallization degree, heterojunctions system and higher charges separation.

4. Conclusions

Visible-light-driven mesoporous Fe_2O_3/TiO_2 microsphere catalysts were successfully synthesized via solvothermal method. The preparation conditions were optimized by orthogonal method of the experimental design, which are reaction temperature at 140 °C, Fe:Ti molar ratio of 0.005:0.01 and amount of glucose about 3.4 g, respectively. The characterized results show that Fe_2O_3 attached on the TiO_2 and formed uniform heterostructured microspheres, which possess high surface area, good crystallinity, and strong visible light absorption. The photocatalytic experiments show that all the as-prepared Fe_2O_3/TiO_2 microspheres have highly photocatalytic activities towards the degradation of RhB under visible light irradiation.

Acknowledgments

This work was financially supported by the National Natural Science Foundation of China (Grant No. 21303130), the Fundamental Research Funds for the Central Universities and Natural Science Basic Research Plan in Shaanxi Province of China (Grant No. 2014JQ2066). Part of SEM work was done at International Center for Dielectric Research (ICDR), Xi'an Jiaotong University, Xi'an, China; the authors also thank Ms. Dai for her help in using SEM and EDX.

Appendix A. Supplementary data

Supplementary data associated with this article can be found, in the online version, at http://dx.doi.org/10.1016/j.apsusc.2014.05.060.

References

[1] A. Fujishima, K. Honda, Nature 238 (1972) 37–38.
[2] M. Addamo, M. Bellardita, D. Carriazo, A.D. Paola, S. Milioto, L. Palmisano, V. Rives, Appl. Catal. B 84 (2008) 742–748.
[3] F.L. Toma, G. Bertrand, S. Begin, C. Meunier, O. Barres, D. Klein, C. Coddet, Appl. Catal. B 68 (2006) 74–84.
[4] M.R. Ghezzar, F. Abdelmalek, M. Belhadj, N. Benderdouche, A. Addou, J. Hazard. Mater. 164 (2009) 1266–1274.
[5] J. Bu, J. Fang, F. Shi, Z. Jiang, W. Huang, Chin. J. Chem. Phys. 23 (2010) 95–101.
[6] J.R. Peller, R.L. Whitman, S. Griffith, P. Harris, C. Peller, J. Scalzitti, J. Photochem. Photobiol. A 186 (2007) 212–217.
[7] M.M. Ren, R. Ravikrishna, K.T. Valsaraj, Environ. Sci. Technol. 40 (2006) 7029–7033.
[8] X.C. Wang, C.Y. Jimmy, C.M. Ho, Y.D. Hou, X.Z. Fu, Langmuir 21 (2005) 2552–2559.
[9] G. Yang, Z. Jiang, H. Shi, M.O. Jones, T. Xiao, P.P. Edwards, Z. Yan, Appl. Catal. B 96 (2010) 458–465.
[10] S. Liu, J. Yu, M. Jaroniec, J. Am. Chem. Soc. 132 (2010) 11914–11916.
[11] J. Ye, W. Liu, J. Cai, S. Chen, X. Zhao, H. Zhou, L. Qi, J. Am. Chem. Soc. 133 (2011) 933–940.
[12] J. Park, E. Kang, S.U. Son, H.M. Park, M.K. Lee, J. Kim, K.W. Kim, et al., Adv. Mater. 17 (2005) 429–434.
[13] G. Yang, T. Xiao, J. Sloan, G. Li, Z. Yan, Chem. Eur. J. 17 (2011) 1096–1100.
[14] Z.Y. Wang, N.S. Ergang, M.A. Al-Daous, A. Stein, Chem. Mater. 17 (2005) 6805–6813.
[15] G. Yang, B. Yang, T. Xiao, Z. Yan, Appl. Surf. Sci. 283 (2013) 402–410.
[16] L.Q. Xiang, X.P. Zhao, J.B. Yin, B.L. Fan, J. Mater. Sci. 47 (2012) 1436–1445.
[17] Q.J. Xiang, J.G. Yu, B. Cheng, H.C. Ong, Chem. Asian J. 5 (2010) 1466–1474.
[18] P. Gao, D.D. Sun, Chem. Asian J. 8 (2013) 2779–2786.
[19] A. Kudo, K. Omori, H. Kato, J. Am. Chem. Soc. 121 (1999) 11459–11467.
[20] Z. He, Y. Li, Q. Zhang, H. Wang, Appl. Catal. B 93 (2010) 376–382.
[21] T.R. Gordon, M. Cargnello, T. Paik, F. Mangolini, R.T. Weber, P. Fornasiero, C.B. Murray, J. Am. Chem. Soc. 134 (2012) 6751–6761.
[22] A.K. Benabbou, Z. Derriche, C. Felix, P. Lejeune, C. Guillard, Appl. Catal. B 76 (2007) 257–263.
[23] J. Du, W. Chen, C. Zhang, Y. Liu, C. Zhao, Y. Dai, Chem. Eng. J. 170 (2011) 53–58.
[24] X.Z. Fu, W.A. Zeltner, M.A. Anderson, Appl. Catal. B 6 (1995) 209.
[25] H. Tada, K. Teranishi, Y. Inubushi, S. Ito, Langmuir 16 (2000) 3304.
[26] H. Haick, Y. Paz, J. Phys. Chem. B 107 (2003) 2319.
[27] M.I. Litter, Appl. Catal. B 23 (1999) 89–114.
[28] G. Yang, Z.F. Yan, T.C. Xiao, B.L. Yang, J. Alloys Compd. 580 (2013) 15–22.
[29] G. Yang, T. Wang, B.L. Yang, Z.F. Yan, S.J. Ding, T.C. Xiao, Appl. Surf. Sci. 287 (2013) 135–142.
[30] S. Kohtani, A. Kudo, T. Sakata, Chem. Phys. Lett. 206 (1993) 116–170.
[31] Y. Liu, L. Yu, C.F. Guo, F.M. Zhang, X.W. (David) Lou, Nanoscale 4 (2012) 183–187.
[32] Y. Liu, L. Zhou, Y. Hu, C.F. Guo, H.S. Qian, F.M. Zhang, X.W. (David) Lou, J. Mater. Chem. 21 (2011) 18359–18364.
[33] G. Yang, Z. Yan, T. Xiao, Appl. Surf. Sci. 258 (2012) 8704–8712.
[34] J.S. Chen, C.P. Chen, J. Liu, R. Xu, S.Z. Qiao, X.W. (David) Lou, Chem. Commun. 47 (2011) 2631–2633.
[35] L.C. Chen, F.R. Tsai, S.H. Fang, Y.C. Ho, Electrochim. Acta 54 (2009) 1304–1311.
[36] M.A. Ahmed, E.E. El-Katori, Z.H. Gharni, J. Alloys Compd. 553 (2013) 19–29.
[37] C.-L. Zhu, H.-L. Yu, Y. Zhang, T.-S. Wang, Q.-Y. Ouyang, L.-H. Qi, Y.-J. Chen, X.-Y. Xue, ACS Appl. Mater. Interfaces 4 (2012) 665–671.
[38] A. Biabani, M. Rezaei, Z. Fattah, J. Nat. Gas Chem. 21 (2012) 415–420.
[39] F. Jia, W. Sun, J.H. Zhang, Y.F. Li, B. Yang, J. Mater. Chem. 22 (2012) 2435–2441.
[40] K.L. Yeung, S.T. Yau, A.J. Maira, J.M. Coronado, J. Soria, P.L. Yue, J. Catal. 219 (2003) 107.
[41] Y. Huo, Y. Jin, J. Zhu, H. Li, Appl. Catal. B 89 (2009) 543–550.
[42] G. Yang, Z. Yan, T. Xiao, Appl. Surf. Sci. 258 (2012) 4016–4022.
[43] G. Yang, Z. Jiang, H. Shi, T. Xiao, Z. Yan, J. Mater. Chem. 20 (2010) 5301–5309.
[44] D. Huang, S. Liao, S. Quan, L. Liu, Z. He, J. Wan, W. Zhou, J. Mater. Res. 22 (2007) 2389–2397.
[45] J. Fang, F. Shi, J. Bu, J. Ding, S. Xu, J. Bao, Y. Ma, Z. Jiang, W. Zhang, C. Gao, W. Huang, J. Phys. Chem. C 114 (2010) 7940–7948.
[46] Z.-H. Zhang, M.F. Hossain, T. Miyazaki, T. Takahashi, Environ. Sci. Technol. 44 (2010) 4741–4746.
[47] K. Sridharan, E. Jang, T.J. Park, Appl. Catal. B 142–143 (2013) 718–728.
[48] M. Mrowetz, W. Balcerski, A.J. Colussi, M.R. Hoffmann, J. Phys. Chem. B 108 (2004) 17269–17273.
[49] C. Xue, T. Wang, G. Yang, B. Yang, S. Ding, J. Mater. Chem. A 2 (2014) 7674–7679.

Please cite this article in press as: T. Wang, et al., Orthogonal synthesis, structural characteristics, and enhanced visible-light photocatalysis of mesoporous Fe_2O_3/TiO_2 heterostructured microspheres, Appl. Surf. Sci. (2014), http://dx.doi.org/10.1016/j.apsusc.2014.05.060